P26

New Methods for Solving the Nonlinear Balance Equation

Qin Xu[1]*, and Jie Cao[2,3]

[1]NOAA/National Severe Storms Laboratory, Norman, Oklahoma

[2]Cooperative Institute for Mesoscale Meteorological Studies, University of Oklahoma

[3]Institute of Atmospheric Physics, China

1. Introduction

The nonlinear balance equation (NBE) can be a very useful dynamic constraint for mesoscale data assimilation because it links the wind or streamfunction field with the mass field more accurately than the geostrophic balance (Charney 1955; Bolin 1956). However, retrieving the streamfunction from the mass field constrained by the NBE remains to be very challenging and largely unsolved since the early attempts traced back to 1950s (Bolin 1955; Miyakoda 1956; Shuman 1957; Arnason 1958; Liao and Zhou 1962; Bijlsma and Hoogendoorn 1983; Wang and Zhang 2003). It is well-known mathematically that the NBE is a special case of the Monge-Amptre's differential equation. If the geostrophic vorticity is larger than $-f/2$ (where f is the Coriolis parameter), the NBE is of the elliptic type with two and only two solutions for given streamfunction boundary values. If the geostrophic-flow vorticity is smaller than $-f/2$ for a constant f in a local area, the NBE becomes locally hyperbolic and this complicates the solution. Because of this complication, there has not been a method of solution for the NBE with the geostrophic vorticity decreased below or even close to $-f/2$ in a local area.

This study reports three recently developed iterative methods. They are developed to attack this problem by rearranging the NBE into a multi-step iterative form based on the leading order balance in the semi-balance model [see (2.13) of Xu 1994]. These methods can solve the NBE efficiently even when the geostrophic-flow vorticity becomes locally smaller than $-f/2$ and thus the equation is no longer elliptic. The three methods are described in Section 2, Idealized experiments are performed in section 3 to examine the effectiveness and accuracy of each method. Application to a hurricane case is presented in Section 4, followed by a summary in section 5.

* Corresponding author address: Qin Xu, National Severe Storms Laboratory, 120 David L. Boren Blvd., Norman, OK 73072-7326; E-mail: Qin.Xu@noaa.gov

2. Methodology

The NBE, $\nabla\cdot(f\nabla\psi) + 2J_{xy}(\partial_x\psi, \partial_y\psi) = \nabla^2\phi$, can be written into the following form:

$$\mathcal{N}(\psi, \phi) \equiv \nabla\cdot(f\nabla\psi) + 2J_{xy}(\partial_x\psi, \partial_y\psi) - \nabla^2\phi = 0,$$

where $\mathcal{N}(\ ,\ )$ denotes the nonlinear differential operator of the NBE, ψ is the nonlinearly balanced streamfunction, and ϕ is the geopotential. The three iterative methods are described in the following subsections.

2.1. Method 1

The NBE can be rewritten into

$$\nabla^2(Z\psi) = \nabla^2(\phi + K) + \nabla\cdot(\psi\nabla Z),$$

where $Z = f + \zeta = f + \nabla^2\psi$, $K = |\nabla\psi|^2/2$, $S = S' + C$, $\nabla^2 S' = \nabla\cdot(\psi\nabla Z)$, $\nabla^2 C = 0$ in D, and $C = Z\psi - (\phi + K + S')$ on ∂D. The iterative procedure performes the follow steps:

a) Start from $k = 0$ and set $\psi_0 = \psi_g \equiv \phi/f$ in D and ∂D.

b) Obtain S'_k as the internally induced solution from $\nabla^2 S'_k = \nabla\cdot(\psi_k\nabla Z_k)$.

c) Obtain C_k as the externally induced solution from $\nabla^2 C_k = 0$ in D with the boundary condition of $C_k = Z_k\psi_k - (\phi + K_k + S'_k)$ on ∂D.

d) Compute $Z_k = f + \nabla^2\psi_k$ and ensure $Z_k \geq 0.5(\nabla^2\phi/f + f)$ (by setting $Z_k = 0.5(\nabla^2\phi/f + f)$ if $Z_k < 0.5(\nabla^2\phi/f + f)$ at any grid points).

e) Update ψ_k to $\psi_{k+1} = (\phi + K_k + S_k)/Z_k$.

f) Go back to step (b) with k increased by 1 until converge.

In the above formulations, $\psi_g \equiv \phi/f$ is the global geostrophic streamfunction (Kuo 1959; Charney and Stern 1962; Schubert et al. 2009). D and ∂D denote the domain and domain boundary, respectively. The internally and externally induced solutions are defined in section 3 of Xu et al. (2011), and these solutions are obtained by using the methods in sections 2-4 of Cao and Xu (2011).

Occasionally, the absolute vorticity Z can become very close to zero or even below zero at a few grid points in a local area. In this case, Z is adjusted locally to the low bound of $0.5(\nabla^2\phi/f + f)$ in step d), so ψ_k can be updated to ψ_{k+1} in step e) without becoming locally and spuriously singular. This low bound can prevent the iterative procedure from divergence but it will cause the converged solution ψ to deviate from the true solution ψ_{True}, locally in and around areas where the true value of Z is below the low bound.

2.2. Method 2

Method 2 is designed to avoid dividing Z directly in step e) of the above method 1. In particular, the above step d) is modified to obtain the increment $\delta\psi_{k+1}$ to update ψ_k to $\psi_{k+1} = \psi_k + \delta\psi_{k+1}$ by minimizing the following cost function:

$$J(\delta\psi_{k+1}) \equiv \iint[(\psi_k+\delta\psi_{k+1})Z_k - (\phi + K_k + S'_k + C_k)]^2 dxdy.$$

2.3. Method 3

Method 3 also uses $\delta\psi_{k+1}$ as the updating variable, but $\delta\psi_{k+1}$ is obtained by solving $\nabla^2(f\delta\psi_{k+1}) = R_k$ in D with $\delta\psi_{k+1} = 0$ on ∂D, where R_k is the residual of the NBE from the previous k^{th} step. Specifically, starting from $k = 0$ with $\psi_0 = \psi_g$, the method performs the following two steps:

a) Obtain $\delta\psi_{k+1}$ by solving

$$\nabla^2(f\delta\psi_{k+1}) = R_k \equiv \mathcal{N}(\psi_k, \phi) \text{ in } D$$

with $\delta\psi_{k+1} = 0$ on ∂D;

b) Update ψ_k to $\psi_{k+1} = \psi_k + \delta\psi_{k+1}$ and go back to step a) until R_k becomes sufficiently small.

By using the identity $\nabla^2(f\psi) = \nabla\cdot(f\nabla\psi) + \nabla\cdot(\psi\nabla f)$, the NBE can be written into the following perturbation form:

$$\nabla^2(f\psi') = \nabla\cdot(\psi\nabla f) - 2J_{xy}(\partial_x\psi, \partial_y\psi),$$

where $\psi' \equiv \psi - \psi_g$ is the ageostrophic streamfunction, that is, the perturbation streamfunction with respect to ψ_g. By setting $\psi = \psi_0 = \psi_g$ with f = constant on the right-hand side, the above perturbation NBE recovers the vertical component of the quasi-geostrophic (QG) C-vector equation in (2.2c) of Xu (1992). This implies that the solution obtained in step a) from the initial guess of $\psi = \psi_0 = \psi_g$, that is, $\delta\psi_1 = \psi_1 = \psi'$ is simply and essentially the QG ageostrophic streamfunction. Thus, the solution $\delta\psi_{k+1}$ obtained in step a) from the updated ψ_k through each subsequent iteration adds an incremental streamfunction (that decreases toward zero as k increases) to the QG ageostrophic streamfunction toward the final solution $\delta\psi \equiv \psi - \psi_g$ where ψ is the nonlinearly balanced streamfunction.

3. Idealized experiments

Idealized experiments are designed first to examine the accuracy and computational efficiency of each method, and to evaluate their effectiveness in overcoming the difficulties caused by the local non-elliptic condition (with $\zeta_g \equiv \nabla^2\psi_g < -f/2$).

Fig. 1 shows the true ψ, denoted by ψ_{True}, constructed analytically, the corresponding ϕ, the geostrophic-flow vorticity $\zeta_g \equiv \nabla^2\psi_g$, and the near-zero residual of the NBE, that is, $\mathcal{N}(\psi_{\text{True}}, \phi)$. Note that ζ_g becomes smaller than $-f/2$ in a small area near the upper-right corner in Fig. 1c.

Fig. 2 shows the solution error defined $\Delta\psi \equiv \psi - \psi_{\text{True}}$ and the residual error $R \equiv \mathcal{N}(\psi, \phi)$ of the NBE for the solution ψ computed by each method. Table 1 shows the correlation coefficient (CC) between $\nabla\cdot(f\nabla\psi) + 2J_{xy}(\partial_x\psi, \partial_y\psi)$ and $\nabla^2\phi$, relative RMS error defined by RRE $\equiv \iint[\mathcal{N}(\psi,, \phi)]^2dxdy/\iint[\nabla\cdot(f\nabla\psi)]^2dxdy$, and the CPU time for each method.

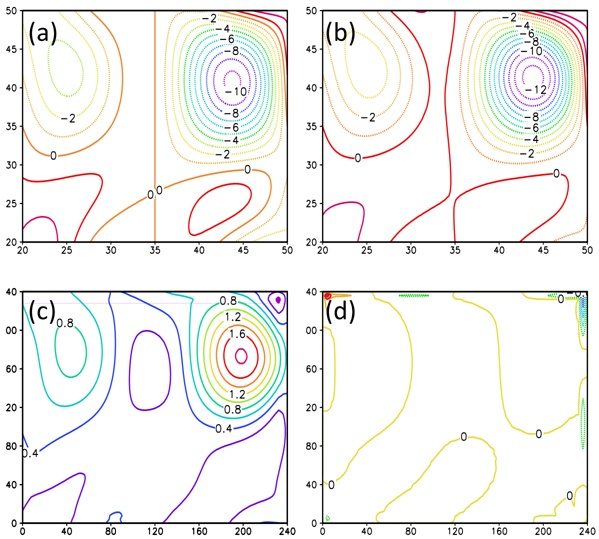

Fig. 1 (a) ψ_{True} (10^6 m^{2}s^{-1}), (b) ϕ (10^2 m^{2}s^{-2}), (c) ζ (10^{-4} s^{-1}), and (d) $\mathcal{N}(\psi_{\text{True}}, \phi)$ (10^{-8} s^{-2}).

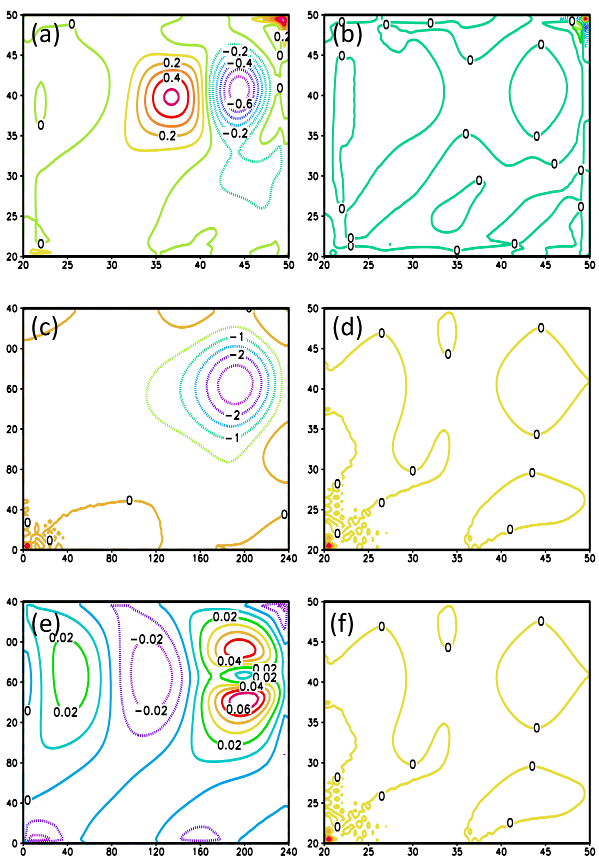

Fig. 2. (a) $\Delta\psi \equiv \psi - \psi_{\text{True}}$ (10^6 m^{2}s^{-1}) for method 1. (b) Residual error $R \equiv \mathcal{N}(\psi, \phi)$ (10^{-8} s^{-2}) for method 1. (c) As in (a) but for method 2, (d) As in (b) but for method 2. (e) As in (a) but for method 3. (f) As in (b) but for method 3.

Table 1. CC, RRE and CPU times for three methods

	CC	RRE	CPU time (s)
TRUE	0.999997	0.00876	
Method 1	0.973981	0.23638	0.27
Method 2	0.975421	0.32888	23.39
Method 3	0.999602	0.02826	7.48

4. Application to real data

Method 3 is used to compute the nonlinearly balanced streamfunction ψ from the geopotential perturbation field ϕ' at 260hPa produced by HWRF 6-hour forecast of Tropical Storm Chantal valid at 1800 UCT on 07/08/2013. The results are shown in Fig. 3 with CC = 0.9997, RRE = 0.02438 and CPU time = 2.19 s.

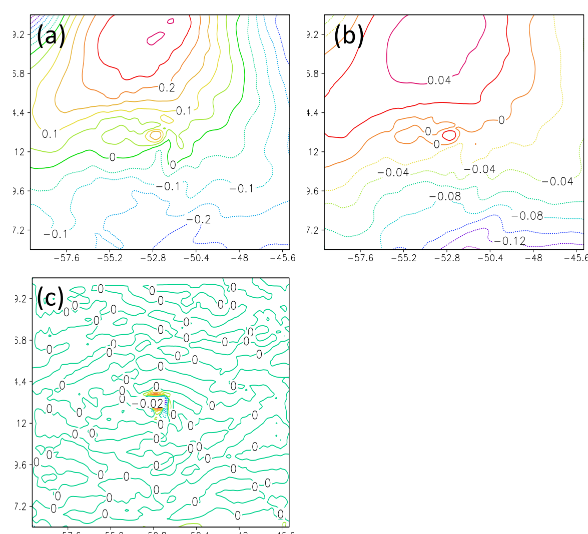

Fig. 3 (a) ϕ' (10^2 m^{2}s^{-2}), (b) ψ (10^7 m^{2}s^{-1}),, and (c) $R \equiv \mathcal{N}(\psi,, \phi)$ (10^{-10} s^{-2}) computed from the HWRF 6-hour forecasted ϕ at 260hPa for Tropical Storm Chantal at 1800 UCT on 07/08/2013.

5. Summary

The three methods have been tested with idealized and real cases in which $\zeta_g \equiv \nabla^2\psi_g$ becomes locally less than $-f/2$. All three methods can work as long as $\zeta_g \equiv \nabla^2\psi_g > -f/2$.

Method 1 is most efficient but least accurate and it requires $Z_k > 0$. Method 2 is least efficient. Method 3 is most accurate in all cases, but it needs a further modification (beyond this study) to improve its applicability to mesoscale flows.

Acknowledgments. The authors are thankful to Drs. Qingfu Liu and Xiaolin Xu at NCEP for providing the HWRF forecast data. The research work was supported by the ONR Grant N000141410281 to the University of Oklahoma (OU). Funding was also provided to CIMMS by NOAA/Office of Oceanic and Atmospheric Research under NOAA-OU Cooperative Agreement #NA17RJ1227, U.S. Department of Commerce. The second author, Dr. Jie Cao, was also supported by the NSF of China (40205033), the National Basic Research Program of China (2012CB417201), and the Supporting Program for Science and Technological Research of China (GYHY201406001).

References.

Arnason, G., 1958: A convergent method for solving the balance equation. *J. Meteor.*, **15**, 220-225.

Bijlsma, S., and R. Hoogendoorn, 1983: A convergence analysis of a numerical method for solving the balance equation. *Mon. Wea. Rev.*, **111**, 997-1001.

Bolin, B., 1955: Numerical forecasting with the barotropic model. *Tellus*, **7**, 27-49.

Bolin, B., 1956: An improved barotropic model and some aspects of using the balance equation for three-dimensional flow. *Tellus*, **8**, 61-75.

Cao, J. and Q. Xu, 2011: Computing streamfunction and velocity potential in a limited domain. Part II: Numerical methods and test experiments. *Adv. Atmos. Sci.*, **28**, 1445-1458.

Charney, J., 1955: The use of the primitive equations of motion in numerical forecasting. *Tellus*, **7**, 22-26.

Charney, J. G., and M. E. Stern, 1962: On the stability of internal baroclinic jets in a rotating atmosphere. *J. Atmos. Sci.*, **19**, 159-172.

Kuo, H. L., 1959: Finite amplitude three-dimensional harmonic waves on the spherical earth. *J. Meteor.*, **16**, 524-534.

Liao, T., and T. Chow, 1962: On the method for solving the balance equation in finite difference form. *Acta Meteor. Sinica*, **32**, 224-231.

Miyakoda, K., 1956: On a method of solving the balance equation. *J. Meteor. Soc. Japan*, **34**, 364-367.

Schubert, W. H., R. K. Taft, and L. G. Silvers, 2009: Shallow water quasi-geostrophic theory on the sphere. *J. Adv. Model. Earth Syst.*, **1**, No. 2, 1-17.

Wang, X., and D. Zhang, 2003: Potential vorticity diagnosis of a simulated hurricane. Part I: Formulation and qusi-balanced flow. *J. Atmos. Sci.*, **60**, 1593-1607.

Xu, Q., 1992: Ageostrophic pseudo-vorticity and geostrophic C-vector forcing – A new look at the Q-vector in three-dimensions. *J. Atmos. Sci.*, **49**, 981–990.

Xu, Q., 1994: Semibalance model—connection between geostrophic-type and balanced-type intermediate models. *J. Atmos. Sci.*, **51**, 953-970.

Xu, Q., J. Cao, and S. Gao, 2011: Computing streamfunction and velocity potential in a limited domain. Part I: Theory and integral formulae. *Adv. Atmos. Sci.*, **28**, 1433-1444.